

Ultrashort Electron Wave Packets via Frequency-Comb Synthesis

Matteo Aluffi,^{1,†} Thomas Vasselon^{1,†} Seddik Ouacel¹ Hermann Edlbauer,¹ Clément Geffroy¹,¹
Preden Roulleau,² D. Christian Glattli² Giorgos Georgiou³,³ and Christopher Bauerle^{1,*}

¹Université Grenoble Alpes, CNRS, Grenoble INP, Institut Néel, Grenoble 38000, France

²Université Paris-Saclay, CEA, CNRS, SPEC, Gif-sur-Yvette 91191, France

³James Watt School of Engineering, Electronics and Nanoscale Engineering,
University of Glasgow, Glasgow G12 8QQ, United Kingdom



(Received 2 January 2023; revised 7 July 2023; accepted 12 July 2023; published 5 September 2023)

Single-electron sources are an essential component of modern quantum nanoelectronic devices. Owing to their high accuracy and stability, they have been successfully employed for metrology applications, studying fundamental matter interactions and more recently for electron quantum optics. They are traditionally driven by state-of-the-art arbitrary wave-form generators that are capable of producing single-electron pulses on the sub-100-ps time scale. In this work, we use an alternative approach for generating ultrashort electron wave packets. By combining several harmonics provided by a frequency comb, we synthesize Lorentzian voltage pulses and then use them to generate electron wave packets. Through this technique, we report on the generation and detection of an electron wave packet with a temporal duration of 27 ps generated on top of the Fermi sea of a two-dimensional electron gas. Electron pulses this short enable studies on elusive ultrafast fundamental quantum dynamics in nanoelectronic systems and may pave the way to implementing flying-electron qubits by means of levitons.

DOI: 10.1103/PhysRevApplied.20.034005

I. INTRODUCTION

Electronic excitations in solid-state nanoelectronic systems provide a unique platform for investigating fundamental matter interactions, such as many-body interactions, the fractional quantum Hall effect, and Fermion statistics, as well as Abelian and non-Abelian statistics [1–10]. The ability to control such excitations at the individual electron level opens up exciting perspectives in terms of quantum information processing and real-time control of topologically protected excitations [4,10,11]. In this respect, the advent of highly efficient and precise single-electron sources has been found to be technologically very important for metrology and more specifically for the definition of the quantum current standard [12–14]. In addition to metrology applications, the quality of these sources has made them very popular in the field of quantum nanoelectronics. They have recently been the driving force for the development of electron quantum optics, where—in analogy to quantum optics—quantum information is encoded in the charge or spin degree of freedom of single propagating electrons [15–22].

There are currently several types of single-electron sources, with the majority of them being based on isolating

electrons in well-defined regions through electrostatic barriers, that can accommodate one or a few electrons, which are then injected into nanoelectronic circuits [19,23–26]. For such single-electron sources, one has to distinguish the following two cases:

(i) The injected electrons have energies of several tens of millielectronvolts, well separated from the bulk electrons. As a consequence, the electron-electron interaction with other electrons in the Fermi sea is suppressed. On the other hand, this makes these systems more prone to decoherence due to fluctuations in the electromagnetic environment such as dopants [19] or due to electron-phonon interactions [27,28]. The main application for these kind of quantum-dot-based sources is in the field of metrology, where current advances report an electron-pumping accuracy of as high as 0.92 ppm (parts per million) [29]. In addition to metrology, their use for electron quantum optics is still an open research topic [16–21].

(ii) The electron is injected from a larger quantum dot into the edge channel of a quantum Hall system [23]. As a consequence, the electrons are emitted much closer to the Fermi sea, typically in the tens-of-microelectronvolts range. As the bandwidth of the wave packet is smaller than the energy of emission, they are still well separated from the Fermi sea and coherent electron transport has already been observed [4].

*Corresponding Author: christopher.bauerle@neel.cnrs.fr

†These authors contributed equally to this work.

An alternative technique for generating single electrons relies on temporally short voltage pulses, also known as levitons. Typically, any voltage signal that is applied on an electron reservoir can induce the motion of free carriers (electrons and holes). It has, however, been postulated by Levitov *et al.* [30,31] that voltage pulses with a Lorentzian profile enable pure-electron excitation without any holes. The amount of excited electrons can be controlled by the amplitude of the pulses and can be tuned such that only a single electron is excited from the reservoir. In contrast to quantum-dot-based sources, levitons are excited very close to the Fermi sea, they do not entangle with their environment, and they can be considered as classical current pulses [32]. The first successfully implemented leviton source [5] enabled experiments on electron tomography [33,34] and time-resolved reconstruction of electron wave functions [35]. In addition, recent theoretical works predict that levitons can be used to study entanglement and nonlocality in Mach-Zehnder interferometers [36,37] or to generate an effective fractional charge $e/2$ [38]. In the form of ultrashort wave packets, levitons are also discussed as a promising approach to generate flying-electron qubits [15,16].

The generation of levitons has been mainly driven by state-of-the-art arbitrary wave-form generators (AWGs) that have the capacity to generate single-electron pulses with a temporal duration as short as 42 ps [34]. Although using an AWG for generating single-electron pulses is a powerful technique, one cannot create very short Lorentzian voltage pulses with sufficient precision due to the limited bandwidth and sampling rate. These AWG limitations degrade the signal quality by generating unwanted hole excitations. With the shortest time scales provided by state-of-the-art AWGs, access to elusive dynamics of low-dimensional systems—such as crystallization and fractionalization [39], dynamic control of interference patterns [40], and spectroscopy of quantum coherent circuits [41]—is so far not possible.

An alternative to the generation of levitons through AWGs is to synthesize Lorentzian-shaped voltage pulses using frequency combs. The discovery of frequency combs has revolutionized optical spectroscopy and metrology in the visible and ultraviolet regions of the electromagnetic spectrum [42]. Although very popular in optics, frequency combs have not been utilized extensively for radio frequencies.

In this paper, we use radio-frequency (rf) frequency combs to synthesize ultrashort Lorentzian voltage pulses that enable stable generation of single-electron levitons. By controlling the amplitude and phase of each harmonic of the comb, we show the capability to finely tune the extent of the charge excitation enabling leviton formation and—more importantly—the precise correction of dispersion from the coaxial line bringing the voltage pulse to the sample. Additionally, we demonstrate that the temporal

duration of levitons is tunable from the continuous limit (sinusoidal waves) down to electron wave packets with 20-ps duration. Finally, we inject the output from our frequency-comb generator into a quantum nanoelectronic device and perform a time-resolved measurement of synthesized Lorentzian voltage pulses *in situ* on a cryogenic setup. This work sets strong foundations for exploring time-resolved ultrafast electron dynamics in solid-state systems and opens up possibilities for a competitive flying-electron qubits technology.

II. ARBITRARY-VOLTAGE-PULSE GENERATION

Any periodic signal can be represented by a Fourier series, which is a linear superposition of orthonormal functions, such as sine waves. As shown in Figs. 1(a) and 1(b), a square pulse (orange curve) is described by, e.g., a series of odd harmonics with a $1/n$ decaying amplitude as a function of the frequency. In the same manner, a Lorentzian pulse (blue curve) can be decomposed into a series of harmonics the amplitude of which falls exponentially. The frequency-comb synthesizer that we demonstrate in this work is now a convenient experimental implementation of this mathematical concept.

Multiple harmonic microwave signals with proper adjustment of amplitude and phase are mixed to obtain a

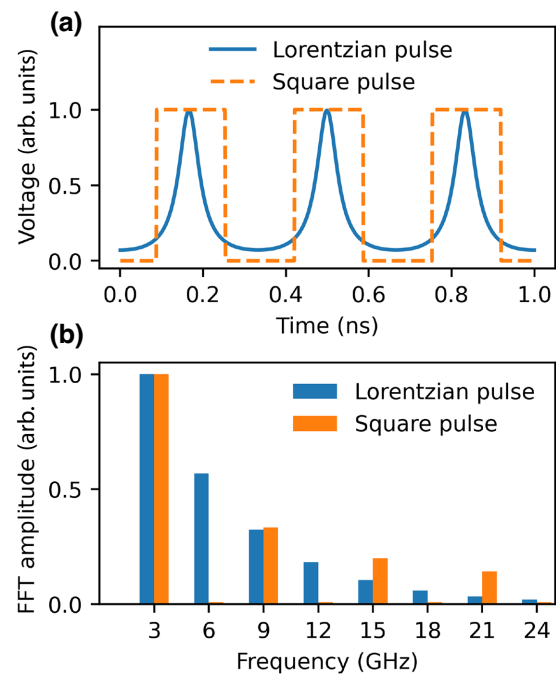


FIG. 1. The principle of Fourier synthesis. (a), (b) The principle of Fourier synthesis explained through a Lorentzian (blue) and a square (orange) voltage pulses. A periodic pulse (a) in the time domain can be decomposed into a series of harmonics in the frequency domain (b), the amplitude and phase of which (not shown here) vary as a function of the frequency.

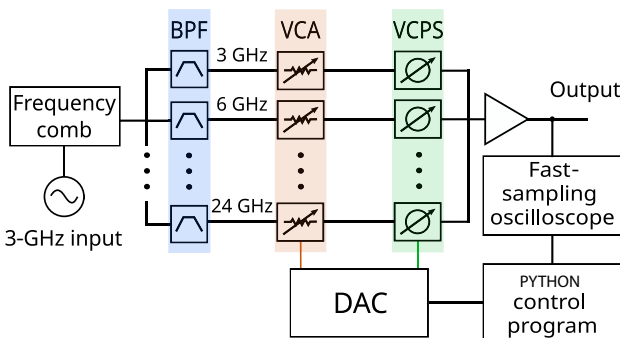


FIG. 2. A block diagram of the arbitrary-voltage-pulse synthesizer. A 3-GHz fundamental frequency is fed through a commercially available frequency comb, which generates higher harmonics. Each harmonic is then selected by a band-pass filter (BPF), attenuated by a voltage-controlled attenuator (VCA), and delayed by the voltage-controlled phase shifter (VCPS). The output is measured in the time domain with a sampling oscilloscope, which provides feedback to home-made control software to automatically tune the VCAs and VCPSs using a programmable digital-to-analog converter (DAC).

Lorentzian target pulse—the central ingredient for leviton formation. As illustrated by the block diagram of Fig. 2, a fundamental sinusoidal signal with a frequency of 3 GHz and a power of 19 dBm is fed into a frequency comb (Marki NLTL-6026). This microwave component is a Schottky-diode-based transmission line with the ability to generate several harmonics from any fundamental frequency up to 50 GHz. After generation, the harmonics are spread into different paths by an eight-way rf splitter. For each path, a 200-MHz bandwidth band-pass filter selects a specific harmonic frequency. The power of each harmonic signal is determined by the selection of microwave components, such as splitters or band-pass filters, giving, for the current implementation, -22.8 dB at 3 GHz to -53.1 dB at 24 GHz. After filtering, each harmonic passes through a voltage-controlled attenuator (VCA) and a voltage-controlled phase shifter (VCPS) that automatically adjust the amplitude and phase for each harmonic signal. Having set the desired harmonic composition, the recombined signal provides the targeted voltage pulse on the output that is finally amplified with a Marki AMZ-40 and measured with a sampling oscilloscope.

The automatic adjustment of the amplitudes and phases is accomplished by a feedback loop. As shown in Fig. 2, the output of our frequency-comb synthesizer is monitored by a digital sampling oscilloscope. The continuously captured data is Fourier transformed and the amplitudes and phases of each harmonic are extracted and compared with the values of the desired pulse. The PYTHON control program then adjusts the voltage applied to the VCAs and VCPSs by means of a dichotomy algorithm. After typically 20 iterations, an almost perfect wave form is obtained.

For a Lorentzian-shape voltage pulse, the optimization algorithm usually converges within a couple of minutes. It is worth noting that adjustment of the attenuators and phase shifters is only needed once and that, as is shown below, the generated pulses are stable over days.

In order to generate leviton pulses in a quantum nanoelectronic device, it is necessary to form Lorentzian charge excitations that carry exactly one or multiple electrons. Accordingly, the voltage-pulse generation must allow for amplitude control that is extremely precise. Figure 3 shows real-time oscilloscope data (black curves) from various synthesized Lorentzian pulses. The traces of Figs. 3(a) and 3(b) show the output for target pulses with durations of 80 ps and 50 ps. Remarkably, they are nearly identical to the theoretical target (blue lines) and have minimum distortion, ensuring the generation of levitons with an extremely low number of hole excitations. The quality of the pulse at zero temperature can be estimated by computing the excess hole excitation, defined as N_h/N_e , where N_h and N_e are the numbers of excited holes and electrons, respectively (see Appendix B). For the 80-ps pulse, a relative hole excitation as low as 0.07% is expected. It is worth noting that voltage pulses with a duration similar to the one illustrated here [Figs. 3(a) and 3(b)] have been used in the past to generate ultrafast levitons, using state-of-the-art AWGs [34,35]. Those voltage pulses resembled more a Gaussian-like pulse rather than the Lorentzian

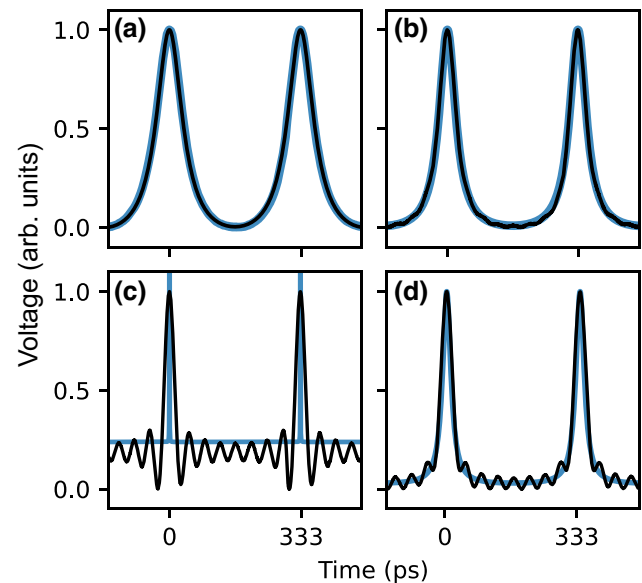


FIG. 3. Voltage pulses generated by the frequency-comb synthesizer. The black solid line corresponds to the pulse measured with a fast oscilloscope and the blue line to the theoretical voltage pulse fed into the optimization algorithm. (a), (b) Lorentzian voltage pulses with duration 80 ps and 50 ps, respectively. (c) The impulse response of the synthesizer, where the input to the optimization algorithm is a delta-like function. (d) The 25 ps Lorentzian voltage pulse used for the measurement in Fig. 5(b).

shape required for the generation of leviton pulses, as demonstrated in Ref. [35].

Analog Fourier synthesis—as demonstrated in this work—enables, on the other hand, the generation of nearly ideal ultrashort Lorentzian pulses that go beyond what state-of-the-art AWGs can achieve. To characterize the limit of our device, we have programmed the synthesizer to output a Dirac-delta-like pulse (a Lorentzian pulse with a width of 0.1 ps). This allows us to measure the impulse response of the system, which can be used to predict the output wave form for any requested input. The output can then be simply computed as a convolution product between the requested input and the impulse response. In our case, the impulse response, shown in Fig. 3(c), is a cardinal sine with a full width at half maximum (FWHM) of 22 ps.

Figure 3(d) illustrates a 25-ps Lorentzian pulse, which appears to be almost identical to its theoretical line shape (blue curve) and with minimal distortion. Even for this case, the generated hole excitations due to the imperfect Lorentzian line shape are less than 0.55% (see Appendix B). The slight distortion observed to either side of the main peak is due to the absence of harmonics higher than 24 GHz. It is worth noting that any limitations imposed by the cutoff frequency of standard SMA connectors used in our setup are automatically compensated by our optimization algorithm, as is any dispersion due to the rf cables.

One of the main advantages of using a frequency-comb-based generator, as opposed to individual phase-locked frequency generators [5], is that all the harmonics are generated from the same source signal. Even if the phase of the fundamental frequency shifts over time, the phases of all higher harmonics will shift in the same manner and therefore the generated signal will not be distorted. The stability of the phase between the harmonics of the synthesizer, as well as their amplitude, is of paramount importance, as any phase or amplitude variation can distort the shape and duration of the generated pulses. This means that for a frequency-comb-based system, an ultrastable picosecond-duration pulse can be synthesized once at the beginning of an experiment and then be kept the same over several days.

The stability of this setup is apparent from the phase and amplitude variation of each harmonic, as shown in Fig. 4. To generate these data, a Lorentzian pulse was measured through a fast oscilloscope, once every 10 min for 50 h. Then, the time-domain data were Fourier transformed, in order to extract the phase and amplitude information for each harmonic. Figure 4(a) shows the phase stability of this synthesizer. In order to have a more meaningful representation of the data, Fig. 4(a) represents the relative time delay of each harmonic with respect to the master frequency (3 GHz). As all higher harmonics are generated from the same master frequency, their relative delay depends only on the passive components used in our setup, such as the filters, attenuators, and phase shifters. The approximately 0.2-ps

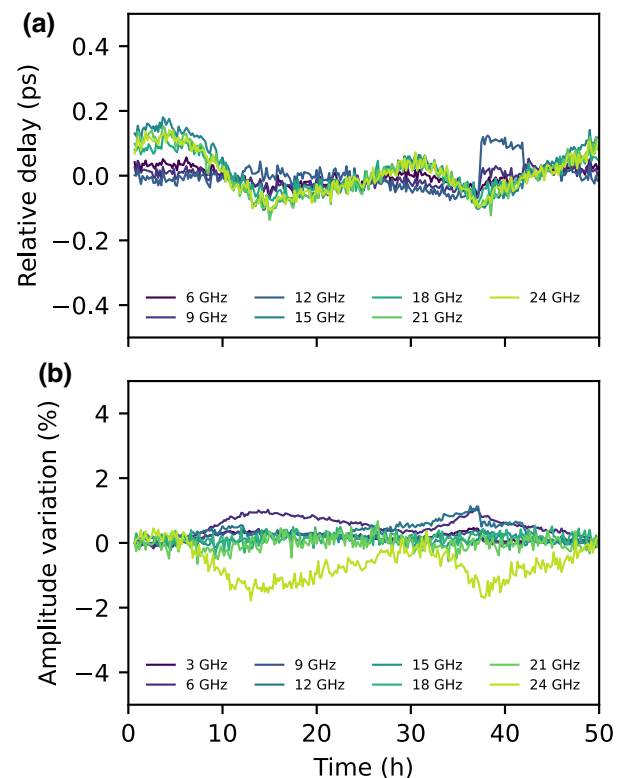


FIG. 4. The output stability over time. The synthesizer output was monitored every 10 min for 50 h. (a) The relative time drift of each harmonic, referenced to the 3-GHz fundamental frequency. (b) The amplitude variation for each harmonic.

delay variation between the harmonics is mainly due to temperature variations in the laboratory over the course of a 2-day period. This relative delay is 2 orders of magnitude smaller than the shortest Lorentzian pulse (25 ps) and can be regarded as negligible.

The amplitude variation of each harmonic is also very stable, as illustrated in Fig. 4(b). The amplitude of each harmonic, besides being important for determining the duration and shape of the final pulse, is also crucial for defining the overall amplitude of the leviton pulses. In order to generate single-electron levitons, it is important to control the amplitude of the generated pulse down to the microvolt level, where indicatively 1 μ V corresponds roughly to the addition of 1% of an extra electron. In this setup, the observed amplitude variation is less than 1% over the 50-h acquisition time and therefore the generated levitons can contain a single electron with a very small uncertainty.

III. GENERATION OF ELECTRON WAVE FUNCTIONS IN A QUANTUM CONDUCTOR

The generation of single-electron leviton pulses relies on voltage pulses with a Lorentzian shape, applied directly on the Fermi sea of a quantum conductor. By perturbing

the Fermi sea with these pulses, we can generate pure-electron excitations, without any holes accompanying the electrons [5,31,33,34], in stark contrast to other popular electron sources [23,24]. This unique property of levitons makes them ideal candidates for flying-electron qubit technologies [16], as well as an attractive platform for studying fundamental time-resolved electron-electron interactions.

To showcase the full potential of our voltage-pulse synthesizer, we demonstrate the generation and time-resolved detection of an electron wave packet with a duration of 27 ps in a two-dimensional electron gas (2DEG). A dilution refrigerator with a base temperature of 20 mK was used to cool down our 2DEG to cryogenic temperatures. The quantum device consists of a Mach-Zehnder interferometer realized by depositing electrostatic surface gates on top of a GaAs/AlGaAs heterostructure, as shown in Fig. 5(a).

The application of a set of negative gate voltages to these electrostatic gates allows engineering of the trajectory of the propagating electron wave packet. For

the time-resolved measurements, only the upper path of the interferometer is used, which means the gate voltages on the central island, as well as the adjacent split wires, are sufficiently negative such that the electron wave packet follows the path indicated by the white dashed line.

To perform time-resolved measurements and reconstruct the electron wave form in the time domain, we split the voltage-pulse output of our synthesizer into two parts using a power divider. The first part, denoted as “Injection” on Fig. 5(a), is sent through a computer-controlled delay line and then into the injection Ohmic contact of our sample [left white square box in Fig. 5(a)]. The second part, denoted as “QPC,” is directly fed into the rf line, which is connected to a quantum point contact (QPC) positioned along the electron wave guide. Both the injection Ohmic contact and the sampling QPC line are equipped with a high-bandwidth bias tee (SHF BT45R) in order to be able to apply a dc and an ac component. For detecting the electrons, we measure the voltage generated across a

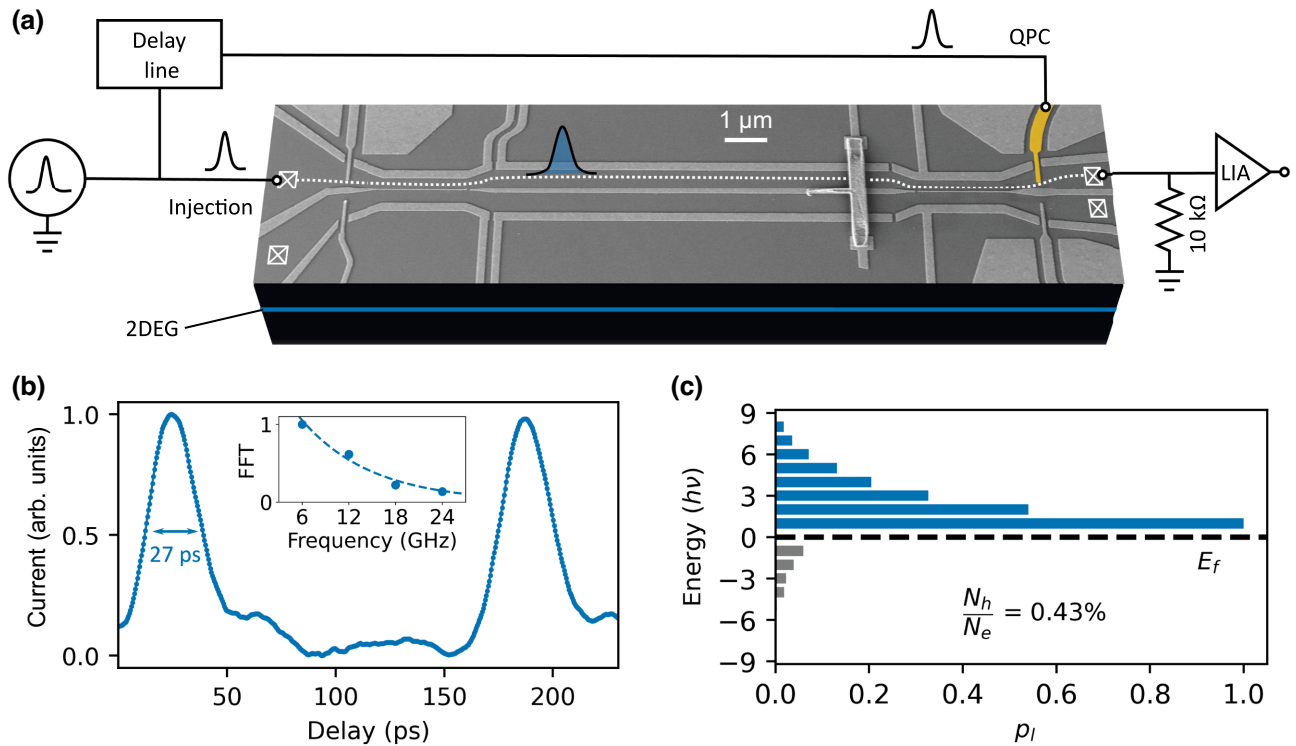


FIG. 5. The time-resolved measurement of an electron wave packet using the frequency-comb synthesizer. (a) A scanning tunneling micrograph of the quantum device made from a GaAs/AlGaAs heterostructure with mobility $\mu_e = 1.77 \times 10^6 \text{ cm}^2 \text{ V}^{-1} \text{ s}^{-1}$ and electron concentration $n_e = 1.92 \times 10^{11} \text{ cm}^{-2}$. The voltage-pulse signal generated with the frequency-comb synthesizer is split into two. One voltage pulse is sent to the upper-left Ohmic contact to launch the electron wave packet, while the second voltage pulse is sent to the QPC (highlighted in yellow) via a mechanical delay line. The QPC is operated as an on-off switch, following the procedure detailed in Ref. [35]. Changing the time delay between the two voltage pulses allows us to reconstruct, in a time-resolved manner, the wave form of the generated electron wave packet. The generated current is detected through a 10-k Ω resistor, amplified at room temperature and measured by a lock-in amplifier (LIA) using a demodulation technique. (b) The time-resolved measurement of a leviton pulse. The inset shows the Fourier transform of the pulse, which follows an exponential trend and therefore confirms the Lorentzian nature of the generated electron wave packet. (c) The calculated excitation spectrum of the electron wave packet generated in (b). $|p_I|^2$ denotes the probability of an electron absorbing or emitting I photons of an energy quanta $\hbar\nu$ (see Appendix B).

10-k Ω resistor, which is then amplified and measured by a lock-in amplifier (LIA). To enable LIA measurements, the “master” source of the synthesizer is modulated at 11.95 kHz.

The QPC line is employed to realize the time-resolved measurement. In line with Roussey *et al.* [35], to reconstruct the time-domain profile of an electron wave packet, the QPC is negatively biased with a sufficient dc voltage such that it blocks all transmission through the waveguide. Then, on top of that dc bias, we apply an ultrashort voltage pulse to the QPC, time delayed by $\Delta\tau$ with respect to the injection pulse. This voltage pulse will effectively act as a switch, enabling transmission for a very short amount of time. By appropriately choosing the negative dc bias, the switching time can be much shorter than the duration of the electron wave packet, therefore enabling accurate reconstruction.

Figure 5(b) is the main result of this paper, showing a sub-30-picoseconds electron wave packet propagating on top of the Fermi sea. In order to benchmark the dispersion of our system, the pulse was generated with a relatively high voltage amplitude and contains around 20 electrons. The dispersion appears to be minimal, as the injected pulse [Fig. 3(d)] had a similar width of 25 ps. To better demonstrate the time-resolved measurement technique, we have used a 6-GHz (166-ps) fundamental frequency for the synthesizer. This has allowed us to measure two pulses within the same scanning window, since the scanning range of our delay line is limited to 230 ps. The Fourier transform of the generated electron wave packet, shown in the inset of Fig. 5(b)], exhibits an exponential behavior, which is distinctive of a Lorentzian electron excitation.

Finally, we analyze the amount of excess hole excitation of the generated Lorentzian voltage pulses as well as the generated electron wave packets by calculating their excitation spectrum at zero temperature in the framework of Floquet scattering theory [43,44] (see Appendix B). The excitation spectrum for the experimentally measured electron wave packet of 27-ps time duration is shown in Fig. 5(c)]. We observe an excess hole excitation that is less than 0.43%. While this is a remarkable result, one needs to bear in mind that this number has been computed at zero temperature. The excess hole excitation for similarly generated Lorentzian pulses at 50 mK has been experimentally measured in Ref. [34] and has been found to be 3%. Since this value is mostly linked to thermal excitation in the Fermi sea, we expect our device to perform similarly at finite temperatures. Similar analyses (see Appendix B) for the generated voltage pulses display an extremely clean excitation spectrum with less than 0.22% hole excitation when the voltage pulses have a duration of 50 ps or more. For the shortest voltage pulses (25 ps), we obtain a maximum of 0.55% hole excitations. Adding additional harmonics in future will allow further improvement of the signal quality as well as shortening of the

generated voltage pulses. With a fundamental frequency of 3 or 6 GHz, the maximum of the harmonic frequencies lies at 36 GHz due to limited frequency bandwidth of the rf components. Within this range, it is possible to generate voltage pulses of a duration down to 14.6 ps. It is possible, on the other hand, to create even shorter voltage pulses, in the range of 1 ps, using an optoelectronic approach [45], but unfortunately their integration at cryogenic temperatures [46] still remains a challenge.

IV. CONCLUSIONS

To conclude, in this paper we have demonstrated a technique for generating levitons (single-electron Lorentzian electron wave packets) based on a frequency-comb synthesizer. Levitons riding on the Fermi sea have been synthesized with a time duration as short as 27 ps. We evaluate the spurious hole contribution to be below 0.43%, which makes these levitons ideal carriers of quantum information in the field of electron quantum optics, as well as for studying fundamental matter interactions in the time domain.

ACKNOWLEDGMENTS

This project has received funding from the European Union H2020 research and innovation program under Grant Agreement No. 862683, “UltraFastNano”. C.B. and D.C.G. acknowledge funding from the French Agence Nationale de la Recherche (ANR), Project Fully Quantum ANR-16-CE30-0015. C.B. acknowledges funding from the French Agence Nationale de la Recherche (ANR), Project ANR QCONTROL ANR-18-JSTQ-0001. C.B., D.C.G., and P.R. acknowledge funding from the French Agence Nationale de la Recherche (ANR), Programmes et Équipements Prioritaire de Recherche (PEPR) Technologies Quantiques, Project E-QUBIT-FLY, ANR-22-PETQ-0012. T.V. acknowledges funding from the French Laboratory of Excellence project “LANEF” (ANR-10-LABX-0051). M.A. acknowledges the MSCA co-fund QuanG Grant No. 101081458, funded by the European Union.

Views and opinions expressed are those of the author(s) only and do not necessarily reflect those of the European Union or the granting authority. Neither the European Union nor the granting authority can be held responsible for them.

APPENDIX A: SYNTHESIZED ELECTRON WAVE PACKETS

To demonstrate the feasibility of generating wave packets containing an arbitrary number of electrons and of any duration, we have performed Fourier synthesis of various Lorentzian pulses with different amplitudes and widths, shown in Figs. 6 and 7. As can be appreciated from the

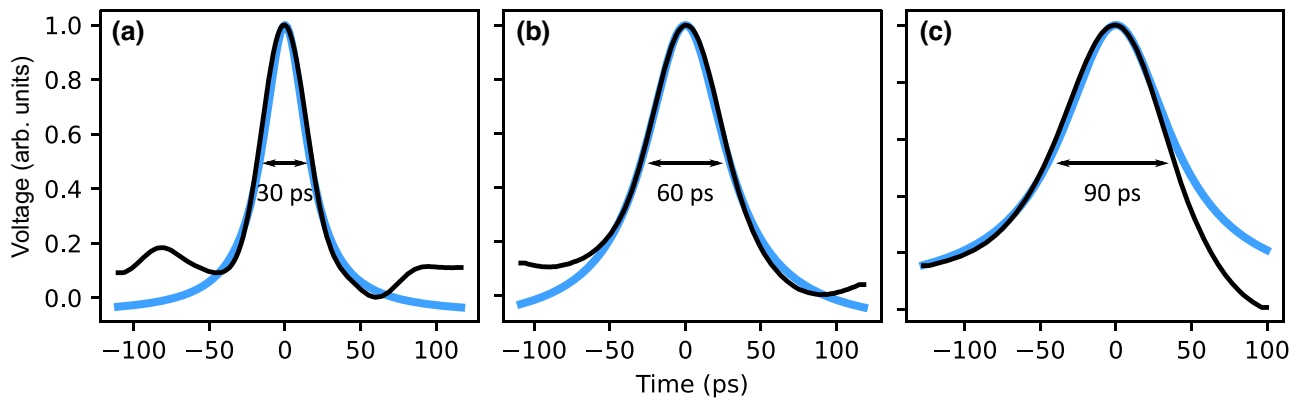


FIG. 6. Synthesized electron wave packets with varying duration, (a) 30 ps, (b) 60 ps, and (c) 90 ps, measured through the 2DEG of the sample shown in Fig. 5. The black lines are experimental data and the blue lines correspond to the best Lorentzian fit.

data, the proposed pulse generator is very versatile, as it allows for the generation of extremely high-quality voltage pulses of any temporal duration and amplitude. As described in the main results of the paper, this is due to the independent tunability of each harmonic and the extreme stability between the frequency-comb harmonics (see Figs. 2 and 4).

One of the greatest challenges of transmitting ultrashort pulses over long rf cables is dispersion. The effect of dispersion is unfortunately more prominent with ultrashort pulses that exhibit a broad spectrum and can result in pulse broadening and chirping (deformation). To be able to generate perfect Lorentzian pulses at cryogenic temperatures (millikelvin), it is important to properly calibrate and precompensate for any dispersion introduced by the transmission lines. By feeding the scattering parameters of the transmission lines into our automated algorithm, we can compensate for the dispersion introduced to our pulse. With this approach, we can automatically take into account for dispersion owing to an arbitrary length of transmission line, therefore having perfect Lorentzian pulses at the sample stage. Both Figs. 6 and 7 are time-resolved

measurements performed through the 2DEG sample, with the method explained in Fig. 5.

APPENDIX B: COMPUTATION OF THE EXCESS HOLE EXCITATION

The excess hole excitation of the generated electron wave packets can be determined by calculating the energy spectrum of each pulse. The electron-hole excitation spectrum due to any periodic voltage pulse applied on the Fermi sea of a quantum conductor can be computed in the framework of Floquet scattering theory [43]. Under the effect of a voltage $V(t)$, the wave function acquires an extra phase term given by

$$\phi(t) = \frac{e}{\hbar} \int_{-\infty}^t V(t') dt', \quad (B1)$$

where e and \hbar are the electron charge and the reduced Planck's constant, respectively, and $V(t)$ is the temporal profile of the applied voltage pulse. In the event of a periodic voltage pulse with repetition frequency ν , the extra phase can be decomposed with the Fourier series

$$\exp(-i\phi(t)) = \sum_{l=-\infty}^{+\infty} p_l \exp(-i2\pi lvt), \quad (B2)$$

where $|p_l|^2$ is the probability of one electron absorbing or emitting l photons. The number of electrons and holes can then be computed as [44]

$$N_e = \sum_{l=1}^{+\infty} l|p_l|^2, \quad (B3)$$

$$N_h = \sum_{l=-\infty}^{-1} (-l)|p_l|^2. \quad (B4)$$

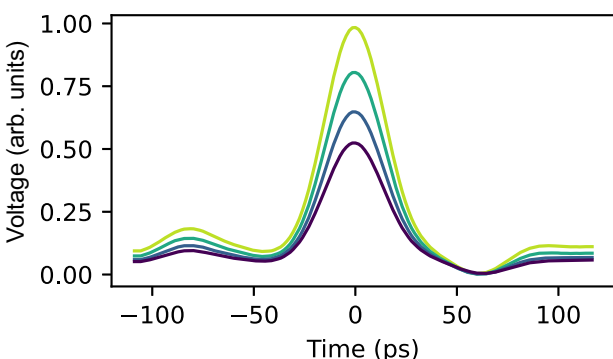


FIG. 7. Synthesized Lorentzian voltage pulses with 30 ps duration, measured through the 2DEG of the sample, shown in Fig. 5. The amplitude of the pulses is varied continuously.

Figure 8 shows the calculated electron-hole excitation spectrum of the generated voltage pulses of Figs. 3(a),

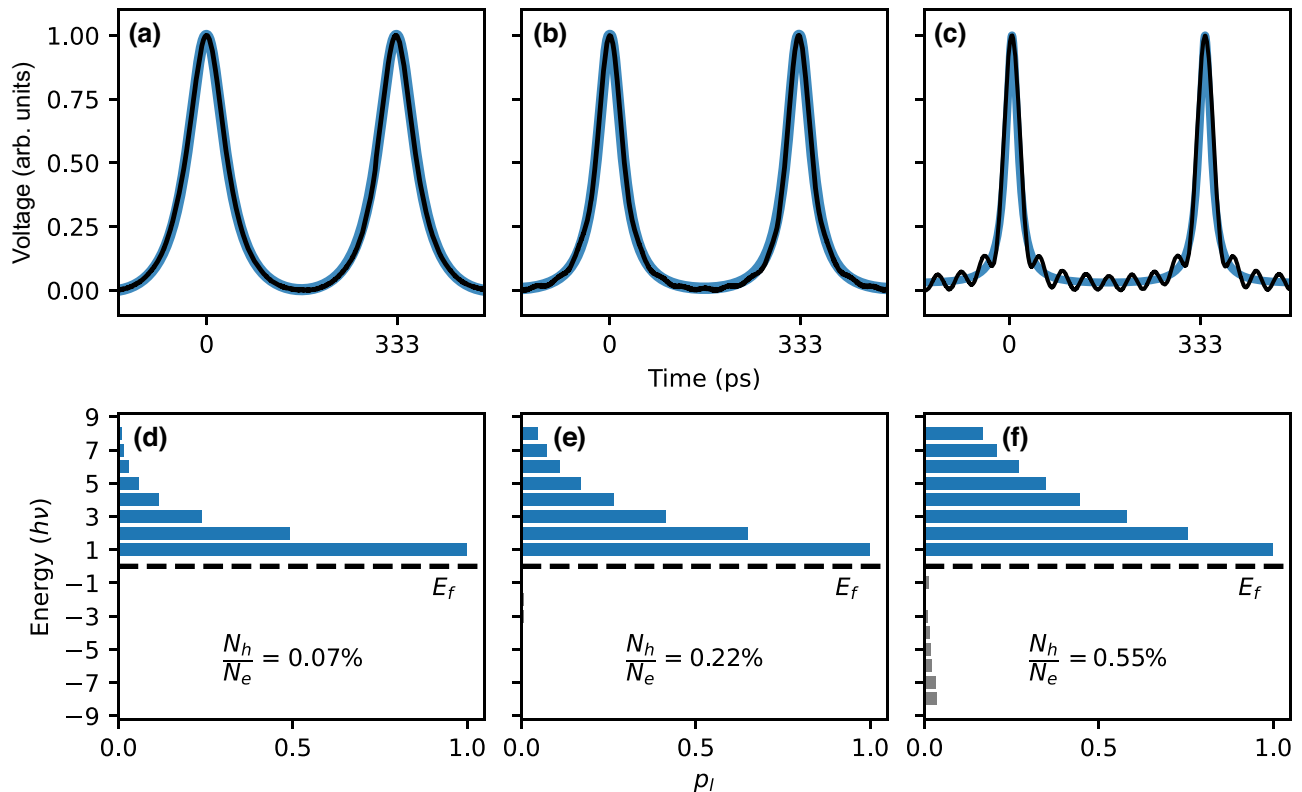


FIG. 8. Excitation spectra of the signal-generator output pulses. (a)–(c) Measured Lorentzian voltage pulses (black) at the signal-generator output with their corresponding Lorentzian fit (blue). The FWHMs are 80 ps, 50 ps, and 25 ps, respectively. (d)–(f) Expected excitation spectra for electron wave packets with same wave form and integer charge per pulse.

3(b), and 3(d). To accurately calculate the excitation spectrum, the amplitude of the measured voltage pulses has been numerically reduced and biased to contain one elementary charge per pulse. The excess hole excitation of each pulse, defined by the ratio of hole-to-electron (N_h/N_e) excitation, is very low and depends on the pulse duration. For long-duration pulses of 80 ps, the ratio of the generated holes to electrons is minimal and in the 0.07% range. This corresponds to the generation of less than one hole for every 10^3 electrons. Reducing the pulse duration to 50 ps increases this ratio slightly to 0.22%, whereas for a 25-ps pulse, the ratio is 0.55%. In Fig. 8(f), we observe an increase in the amount of generated holes for large harmonics (i.e., $\hbar\nu = -9$). This effect is well matched to our theory and it is due to the lack of higher harmonics when synthesizing short Lorentzian voltage pulses. As explained in the main text and shown in Fig. 8(c), this also translates into satellite oscillations on either side of the main pulse.

Analyzing the energy spectrum of the generated electron wave packets, using the Floquet scattering theory, provides quick information on the amount of holes contained within a wave packet. However, while this approach is faster than a tomography experiment, it cannot provide any additional information on whether the electrons contained

within the wave packet are in a pure or mixed quantum state [34].

- [1] A. Stern, Anyons and the quantum Hall effect—A pedagogical review, *Ann. Phys. Jan. Spec. Issue* **2008** *323*, 204 (2008).
- [2] W. D. Oliver, J. Kim, R. C. Liu, and Y. Yamamoto, Hanbury Brown and Twiss-type experiment with electrons, *Science* **284**, 299 (1999).
- [3] M. Henny, S. Oberholzer, C. Strunk, T. Heinzel, K. Ensslin, M. Holland, and C. Schönenberger, The fermionic Hanbury Brown and Twiss experiment, *Science* **284**, 296 (1999).
- [4] E. Bocquillon, V. Freulon, J.-M. Berroir, P. Degiovanni, B. Plaçais, A. Cavanna, Y. Jin, and G. Fèvre, Coherence and indistinguishability of single electrons emitted by independent sources, *Science* **339**, 1054 (2013).
- [5] J. Dubois, T. Jullien, F. Portier, P. Roche, A. Cavanna, Y. Jin, W. Wegscheider, P. Roulleau, and D. C. Glattli, Minimal-excitation states for electron quantum optics using levitons, *Nature* **502**, 659 (2013).
- [6] V. Freulon, A. Marguerite, J.-M. Berroir, B. Plaçais, A. Cavanna, Y. Jon, and G. Fèvre, Hong-Ou-Mandel experiment for temporal investigation of single-electron fraction-alization, *Nat. Commun.* **6**, 6854 (2015).

- [7] M. Kapfer, P. Roulleau, M. Santin, I. Farrer, D. A. Ritchie, and D. C. Glattli, A Josephson relation for fractionally charged anyons, *Science* **363**, 846 (2019).
- [8] H. Bartolomei, M. Kumar, R. Bisognin, A. Marguerite, J.-M. Berroir, E. Bocquillon, B. Plaçais, A. Cavanna, Q. Dong, U. Gennser, Y. Jin, and G. Fèvre, Fractional statistics in anyon collisions, *Science* **368**, 173 (2020).
- [9] J. Nakamura, S. Liang, G. C. Gardner, and M. J. Manfra, Direct observation of anyonic braiding statistics, *Nat. Phys.* **16**, 931 (2020).
- [10] I. Taktak, M. Kapfer, J. Nath, P. Roulleau, M. Acciai, J. Splettstoesser, I. Farrer, D. A. Ritchie, and D. C. Glattli, Two-particle time-domain interferometry in the fractional quantum Hall effect regime, *Nat. Commun.* **13**, 5863 (2022).
- [11] H. Kamata, H. Irie, N. Kumada, and K. Muraki, Time-resolved measurement of ambipolar edge magnetoplasmon transport in InAs/InGaSb composite quantum wells, *Phys. Rev. Res.* **4**, 033214 (2022).
- [12] S. P. Giblin, E. Mykkänen, A. Kemppinen, P. Immonen, A. Manninen, M. Jenei, M. Möttönen, G. Yamahata, A. Fujiwara, and M. Kataoka, Realisation of a quantum current standard at liquid helium temperature with sub-ppm reproducibility, *Metrologia* **57**, 025013 (2020).
- [13] H. Scherer and H. W. Schumacher, Single-electron pumps and quantum current metrology in the revised SI, *Ann. Phys.* **531**, 1800371 (2019).
- [14] N.-H. Kaneko, S. Nakamura, and Y. Okazaki, A review of the quantum current standard, *Meas. Sci. Technol.* **27**, 032001 (2016).
- [15] C. Bäuerle, D. C. Glattli, T. Meunier, F. Portier, P. Roche, P. Roulleau, S. Takada, and X. Waantal, Coherent control of single electrons: A review of current progress, *Rep. Prog. Phys.* **81**, 056503 (2018).
- [16] H. Edlbauer, *et al.*, Semiconductor-based electron flying qubits: Review on recent progress accelerated by numerical modelling, *EPJ Quantum Technol.* **9**, 00 (2022).
- [17] S. Takada, H. Edlbauer, H. V. Lepage, J. Wang, P.-A. Mortemousque, G. Georgiou, C. H. W. Barnes, C. J. B. Ford, M. Yuan, P. V. Santos, X. Waantal, A. Ludwig, A. D. Wieck, M. Urdampilleta, T. Meunier, and C. Bäuerle, Sound-driven single-electron transfer in a circuit of coupled quantum rails, *Nat. Commun.* **10**, 4557 (2019).
- [18] J. Wang, S. Ota, H. Edlbauer, B. Jadot, P.-A. Mortemousque, A. Richard, Y. Okazaki, S. Nakamura, A. Ludwig, A. D. Wieck, M. Urdampilleta, T. Meunier, T. Kodera, N.-H. Kaneko, S. Takada, and C. Bäuerle, Generation of a Single-Cycle Acoustic Pulse: A Scalable Solution for Transport in Single-Electron Circuits, *Phys. Rev. X* **12**, 031035 (2022).
- [19] J. Wang, H. Edlbauer, A. Richard, S. Ota, W. Park, J. Shim, A. Ludwig, A. Wieck, H.-S. Sim, M. Urdampilleta, T. Meunier, T. Kodera, N.-H. Kaneko, H. Sellier, X. Waantal, S. Takada, and C. Bäuerle, Coulomb-mediated antibunching of an electron pair surfing on sound, *Nat. Nanotechnol.* **18**, 721 (2023).
- [20] N. Ubbelohde, L. Freise, E. Pavlovska, P. G. Silvestrov, P. Recher, M. Kokainis, G. Barinovs, F. Hohls, T. Weimann, K. Pierz, and V. Kashcheyevs, Two electrons interacting at a mesoscopic beam splitter, *Nat. Nanotechnol.* **18**, 733 (2023).
- [21] J. D. Fletcher, W. Park, S. Ryu, P. See, J. P. Griffiths, G. A. C. Jones, I. Farrer, D. A. Ritchie, H.-S. Sim, and M. Kataoka, Time-resolved Coulomb collision of single electrons, *Nat. Nanotechnol.* **18**, 727 (2023).
- [22] B. Jadot, P.-A. Mortemousque, E. Chanrion, V. Thiney, A. Ludwig, A. D. Wieck, M. Urdampilleta, C. Bäuerle, and T. Meunier, Distant spin entanglement via fast and coherent electron shuttling, *Nat. Nanotechnol.* **16**, 570 (2021).
- [23] G. Fèvre, A. Mahe, J.-M. Berroir, T. Kontos, B. Placais, D. C. Glattli, A. Cavanna, B. Etienne, and Y. Jin, An on-demand coherent single-electron source, *Science* **316**, 1169 (2007).
- [24] M. D. Blumenthal, B. Kaestner, L. Li, S. Giblin, T. J. B. M. Janssen, M. Pepper, D. Anderson, G. Jones, and D. A. Ritchie, Gigahertz quantized charge pumping, *Nat. Phys.* **3**, 343 (2007).
- [25] S. Hermelin, S. Takada, M. Yamamoto, S. Tarucha, A. D. Wieck, L. Saminadayar, C. Bäuerle, and T. Meunier, Electrons surfing on a sound wave as a platform for quantum optics with flying electrons, *Nature* **477**, 435 (2011).
- [26] R. P. G. McNeil, M. Kataoka, C. J. B. Ford, C. H. W. Barnes, D. Anderson, G. A. C. Jones, I. Farrer, and D. A. Ritchie, On-demand single-electron transfer between distant quantum dots, *Nature* **477**, 439 (2011).
- [27] C. Emary, L. A. Clark, M. Kataoka, and N. Johnson, Energy relaxation in hot electron quantum optics via acoustic and optical phonon emission, *Phys. Rev. B* **99**, 045306 (2019).
- [28] L. A. Clark, M. Kataoka, and C. Emary, Mitigating decoherence in hot electron interferometry, *New J. Phys.* **22**, 103031 (2020).
- [29] G. Yamahata, S. P. Giblin, M. Kataoka, T. Karasawa, and A. Fujiwara, Gigahertz single-electron pumping in silicon with an accuracy better than 9.2 parts in 10⁷, *Appl. Phys. Lett.* **109**, 013101 (2016).
- [30] L. S. Levitov, H. Lee, and G. B. Lesovik, Electron counting statistics and coherent states of electric current, *J. Math. Phys.* **37**, 4845 (1996).
- [31] J. Keeling, I. Klich, and L. S. Levitov, Minimal Excitation States of Electrons in One-Dimensional Wires, *Phys. Rev. Lett.* **97**, 116403 (2006).
- [32] D. Ferraro, B. Roussel, C. Cabart, E. Thibierge, G. Fèvre, C. Grenier, and P. Degiovanni, Real-Time Decoherence of Landau and Levitov Quasiparticles in Quantum Hall Edge Channels, *Phys. Rev. Lett.* **113**, 166403 (2014).
- [33] T. Jullien, P. Roulleau, B. Roche, A. Cavanna, Y. Jin, and D. C. Glattli, Quantum tomography of an electron, *Nature* **514**, 603 (2014).
- [34] R. Bisognin, A. Marguerite, B. Roussel, M. Kumar, C. Cabart, C. Chapdelaine, A. Mohammad-Djafari, J.-M. Berroir, E. Bocquillon, B. Plaçais, A. Cavanna, U. Gennser, Y. Jin, P. Degiovanni, and G. Fèvre, Quantum tomography of electrical currents, *Nat. Commun.* **10**, 3379 (2019).
- [35] G. Roussely, E. Arrighi, G. Georgiou, S. Takada, M. Schalk, M. Urdampilleta, A. Ludwig, A. D. Wieck, P. Armagnat, T. Kloss, X. Waantal, T. Meunier, and C. Bäuerle, Unveiling the bosonic nature of an ultrashort few-electron pulse, *Nat. Commun.* **9**, 2811 (2018).

- [36] A. A. Vyshnevyy, A. V. Lebedev, G. B. Lesovik, and G. Blatter, Two-particle entanglement in capacitively coupled Mach-Zehnder interferometers, *Phys. Rev. B* **87**, 165302 (2013).
- [37] D. Dasenbrook, J. Bowles, J. B. Brask, P. P. Hofer, C. Flindt, and N. Brunner, Single-electron entanglement and nonlocality, *New J. Phys.* **18**, 043036 (2016).
- [38] M. Moskalets, Fractionally Charged Zero-Energy Single-Particle Excitations in a Driven Fermi Sea, *Phys. Rev. Lett.* **117**, 046801 (2016).
- [39] F. Ronetti, L. Vannucci, D. Ferraro, T. Jonckheere, J. Rech, T. Martin, and M. Sassetto, Crystallization of levitons in the fractional quantum Hall regime, *Phys. Rev. B* **98**, 075401 (2018).
- [40] B. Gaury and X. Waintal, Dynamical control of interference using voltage pulses in the quantum regime, *Nat. Commun.* **5**, 3844 (2014).
- [41] P. Burset, J. Kotilahti, M. Moskalets, and C. Flindt, Time-domain spectroscopy of mesoscopic conductors using voltage pulses, *Adv. Quantum Technol.* **2**, 1900014 (2019).
- [42] T. Udem, R. Holzwarth, and T. W. Hänsch, Optical frequency metrology, *Nature* **416**, 233 (2002).
- [43] M. Moskalets and M. Büttiker, Floquet scattering theory of quantum pumps, *Phys. Rev. B* **66**, 205320 (2002).
- [44] J. Dubois, T. Jullien, C. Grenier, P. Degiovanni, P. Rouleau, and D. C. Glattli, Integer and fractional charge Lorentzian voltage pulses analyzed in the framework of photon-assisted shot noise, *Phys. Rev. B* **88**, 085301 (2013).
- [45] D. H. Auston, Picosecond optoelectronic switching and gating in silicon, *Appl. Phys. Lett.* **26**, 101 (1975).
- [46] G. Georgiou, C. Geffroy, C. Bäuerle, and J.-F. Roux, Efficient three-dimensional photonic–plasmonic photoconductive switches for picosecond THz pulses, *ACS Photon.* **7**, 1444 (2020).